

Axial compression behavior of circular recycled concrete-filled steel tubular short columns reinforced by silica fume and steel fiber

Juan Chen^a, Xuan Liu, Hongwei Liu and Lei Zeng^{*}

School of Urban Construction, Yangtze University, 1 Nanhuan Road, Jingzhou, Hubei, China

(Received August 8, 2017, Revised December 8, 2017, Accepted February 25, 2018)

Abstract. This paper presents an experimental work for short circular steel tube columns filled with normal concrete (NAC), recycled aggregate concrete (RAC), and RAC with silica fume and steel fiber. Ten specimens were tested under axial compression to research the effect of silica fume and steel fiber volume percentage on the behavior of recycled aggregate concrete-filled steel tube columns (RACFST). The failure modes, ultimate loads and axial load-strain relationships are presented. The test results indicate that silica fume and steel fiber would not change the failure mode of the RACFST column, but can increase the mechanical performances of the RACFST column because of the filling effect and pozzolanic action of silica fume and the confinement effect of steel fiber. The ultimate load, ductility and energy dissipation capacity of RACFST columns can exceed that of corresponding natural aggregate concrete-filled steel tube (NACFST) column. Design formulas EC4 for the load capacity NACFST and RACFST columns are proposed, and the predictions agree well with the experimental results from this study.

Keywords: recycled concrete-filled steel tube (RACFST); axial compression; steel fiber reinforced concrete; mechanical performance

1. Introduction

Recycled coarse aggregate (RCA) has been used as a partial replacement of the natural coarse aggregate (NCA) for a number of years. In recent years a lot of studies have been published about the use of RCA in structural concrete (Manzi *et al.* 2013, Seara-Paz *et al.* 2016, Thomas *et al.* 2016, Lotfy and Al-Fayez 2015) non-structural concrete (Rodríguez *et al.* 2016, Mas *et al.* 2012) and road construction (Engelsen *et al.* 2017, Agrela *et al.* 2012, Engelsen *et al.* 2012). The results indicated that the quality of RCA is lower than that of NCA, due to the higher absorption, adhered mortar and the impurities that limit their use.

To promote the usage of RCA and improve the mechanical strength and stiffness of RAC, some researchers use the RAC as the concrete fill of concrete-filled steel tube (CFST) to form RACFST. The mechanical performances of RACFST have been explored in several studies. Researchers have mostly focused on the axial response of circular RACFST stub columns (Konno *et al.* 1997, 1998, Qiu *et al.* 2011, Chen *et al.* 2010a and b, Chen 2011, Yang and Han 2006a and b, Niu and Cao 2015, Wang *et al.* 2015, Ma and Wang 2012). These findings indicate that the failure mode and mechanical properties of RACFST columns are identical with that of the corresponding natural aggregate concrete-filled steel tubular (NACFST) columns. Some

researchers ignored the high water absorption of the RCA, which lead to the different results on the load capacity of the RACFST columns. But the RCA replacement ratio has little effect on the load capacity of the RACFST stub columns. Zhang *et al.* (2012) reported experimental studies on the slender columns of RACFST under axial loading. Chen *et al.* (2012) examined the behavior of eccentrically loaded circular RACFST slender columns. Zhang (2011), Chen *et al.* (2017), Zhang *et al.* (2014), Yang *et al.* (2009), Wu *et al.* (2012, 2013) conducted the experimental work on the performance of RACFST columns under cyclic loading. Xu *et al.* (2017) simulate the seismic behavior of square RACFST columns. The studies show that RACFST is a practical structural application of RAC, and it exhibits an efficient way of reducing the adverse impact on the natural environment caused by the RCA.

The previous studies almost all considered the effect of replacement percentage of RAC on the mechanical properties of the RCAFST, the replacement percentage of RAC ranging from 0% to 100%. In order to maximize the utilization of recycled aggregate in RCAFST structure, we should study the mechanical performance of RCAFST with 100% RCA. However, the studies on the RCAFST with 100% RAC are relatively recent, and those on the silica fume and steel fiber reinforced RCAFST with 100% RAC are especially lacking.

In this paper we conducted experimental tests to investigate the reinforcing effect of silica fume and steel fibers on the short RACFST columns. Ten specimens, including two NACFST specimens and eight RACFST specimens with and without silica fume and steel fiber, were tested under axial load. The failure modes, ultimate

*Corresponding author, Professor,
E-mail: zenglei@yangtzeu.edu.cn

^a Ph.D., E-mail: chenjuan9876@163.com

Table 1 Parameters of specimens

Specimens	L (mm)	t (mm)	D (mm)	L/D	f_y (MPa)	f_{cu} (MPa)	ζ
C-0-0	390	4.1	133	2.93	299.7	79.17	0.68
C-100-0	390	4.1	133	2.93	299.7	65.64	0.82
C-100-0.5	390	4.1	133	2.93	299.7	72.84	0.74
C-100-1.0	390	4.1	133	2.93	299.7	80.64	0.66
C-100-1.5	390	4.1	133	2.93	299.7	79.09	0.68

Table 2 Properties of coarse aggregate

Type	Particle size (mm)	Bulk density ($\text{kg}\cdot\text{m}^{-3}$)	Water absorption rate	Crushing value
NA	5~20	1486	0.5%	9.6%
RA	5~20	1314	5.0%	16.4%

loads and axial load-axial strain relationships were obtained from the tests. The confined concrete strength is calculated based on the experimental results. The effects of the silica fume and steel fiber volume percentage on the ultimate load of RACFST columns, confined concrete strength are discussed in this paper. Furthermore, Design formulas are proposed to predict the load capacity of RACFST with and without silica fume and steel fiber.

2. Experimental descriptions

2.1 Test specimens

Ten RACFST short columns, including two NACFST columns, were tested under axial load. The influence of silica fume and steel fiber were considered in this investigation. The details of all specimens are summarized in Table 1. The ten specimens include two identical specimens from each type. The specimens are labeled as follows: letter C represents the circular cross section. The following numbers represent the replacement ratio of coarse aggregate and steel fiber volume percentage, respectively. In Table 1, Letter L is the length of the specimens, D is the external diameter of the steel tube, t is the thickness of steel tube, f_{cu} is the 100 mm cubic compressive strength of concrete, f_y is the yield strength of steel tube, ζ is the steel tube confinement index, $\zeta = A_s f_y / A_c f_c$ (A_s , A_c , f_c refers to the cross-sectional area of steel pipe, the cross-sectional area of concrete, the axial compressive strength of concrete, respectively. $f_c = 0.95 \times 0.8 f_{cu}$).

2.2 Material properties

The concrete mixtures were made with Portland cement, river sand, natural or recycled coarse aggregate, silica fume and steel fiber. Super-plasticizer was used to ensure a good workability. Ordinary Portland cement with a 28 d compressive strength of 42.5 MPa was used in this experiment. The fine aggregate was river sand with fineness modulus of 2.8. The NCA and RCA were washed for several times and NCA dried out naturally, RCA dried in drying oven. The RCA were obtained from the concrete block crushed by hammer crushers. The original design strength of these concrete was C70. The particle size of RCA was 5-10 mm and 10-20 mm with ratio of 3:7. The basic properties of coarse aggregate are shown in Table 2.

The steel tubes of all specimens were fabricated from seamless circular steel tubes. One tube diameter of 133 mm was used. The average values of yield strength, ultimate tensile strength and elastic modulus for the steel tubes were 299.7 MPa, 433.5 MPa and 205 GPa, respectively.

A hooked-end type steel fiber was used in the concrete mixtures. The steel fibers had a length of 30 mm, diameter of 0.52 mm, aspect ratio of 57.6, and density of 7850 kg/m^3 . The tensile strength of the steel fiber, as provided by the manufacturer, was larger than 1060 MPa. Steel fiber reinforced concrete with three different volume percentages of 0.5%, 1.0% and 1.5% were used as infilling.

Silica fume obtained from a factory in China was used as a mineral admixture in concrete production. Cement was replaced with silica fume of 10% weight.

Four kinds of recycled aggregate concrete were made according to proportioning of reference concrete compounded with natural aggregate. The mix designs for concrete are shown in Table 3. Taking into account that the water absorption of recycled aggregate is 10 times of the natural aggregate, the mixed water in each RAC group needs to be recalculated. In order to eliminate the effect of decreased water binder ratio caused by recycled aggregate

Table 3 Mix of concrete

Number	Cement (kg/m^3)	Water (kg/m^3)	Silica fume (kg/m^3)	Sand (kg/m^3)	NCA (kg/m^3)	RCA (kg/m^3)	Steel fiber (kg/m^3)
C-0-0	500	150	0	595	1155	0	0
C-100-0	500	202.0	0	595	0	1155	0
C-100-0.5	450	198.8	50	665	0	1085	39.7
C-100-1.0	450	198.8	50	665	0	1085	78.5
C-100-1.5	450	198.8	50	665	0	1085	117.9

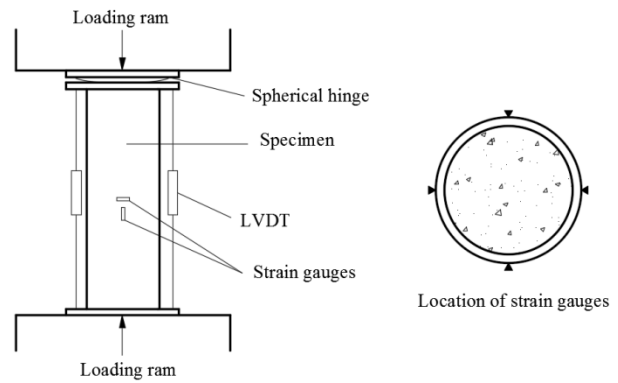


Fig. 1 Testing and measuring apparatus

water absorption on the strength of recycled concrete. The water consumption must consist of two parts. One part is calculated by water-binder ratio of 0.3, the other part is additional water according to the calculation of water absorption of recycled coarse aggregate.

2.3 Specimens preparation

Prior to filling the concrete, the ends of each tube specimen were machined to insure maximum uniformity of contact with the loading heads of the testing machine, and steel plates with thickness of 10 mm were welded to bottom ends of the steel tubes to restrict the concrete during casting. The steel tubes were filled with concrete in one layer and then carefully compacted. Finally all specimens were adopted with natural curing for 150 days before loading. For each batch of concrete, sets of concrete cubes with the side length of 100 mm were cast. These cubes were tested after being cured in water at the time of ultimate tests to evaluate the concrete compressive strength.

2.4 Test set-up

Before the test, the top ends of the columns were polished smoothly with grinder, so that the steel tube and the concrete core can be loaded simultaneously during testing. In addition, a spherical hinge was placed on the top end of the column when tested to ensure specimens were under axial compression. Fig. 1 gives a general view of the test setups.

All specimens were tested under a computer controlled electro hydraulic servo universal testing machine with a capacity of 5000 kN in Civil Engineering Experiment

Center of Yangtze University. The load was applied in an increment of 50 kN before load reaching 75% of the maximum load. Each load interval was maintained for about 2 min and at each load increment the strain readings and the deflection measurements were recorded. Then the axial compressive load was continually increased, the tests were terminated when the bearing capacity of stub columns decreases to 85% of maximum load, or specimens were damaged with significant deformation and steel pipe wrinkling.

Two LVDTs with the range of ± 25 mm were located vertically to measure the axial shortening of the specimens. Eight strain gauges were placed at the mid-height of the steel tube to measure the vertical deformation and perimeter expansion at four symmetric locations.

3. Test result and analysis

3.1 Failure modes and test observations

All specimens were tested to failure under axial compression. It was found that all stub columns had good deformation-resistance ability and post-peak load-bearing capacity. During the loading process, there is no obvious deformation at the early stage of loading. When the applied load reached 90% of the ultimate load, the iron corrosion began to fall from the tube wall. With a further increase of load, visible local buckling on the columns appeared. While the load increased continually, the deformation of the specimen increased, the local shear slip line appeared on the wall of the steel tube and the outer surface bulked about 1-3 mm in annular direction. After reaching the ultimate



C-0-0



C-100-0



C-100-0.5



C-100-1.0



C-100-1.5

Fig. 2 Failure mode of specimens

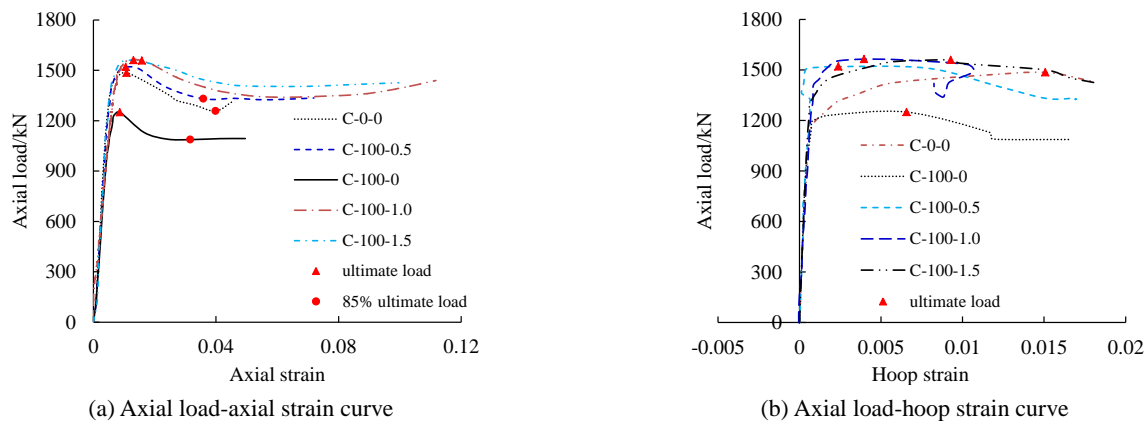


Fig. 3 Axial load–strain behavior of all specimens

strength, the bearing capacity of specimens declined, but the reduction was not too much. At the same time, the deformation of specimens increased continuously.

All specimens present shear failure of the concrete core. The steel tube presents local buckling failure, which is shown in Fig. 2. The addition of steel fiber and silica fume would not change the failure mode. This is because that the steel fiber will work only after the appearance of cracking.

3.2 Ultimate load

The maximum load during loading is defined as the ultimate load. The ultimate loads of the specimens are shown in Table 4. The results show that the coarse aggregate was all replaced by RCA will decrease the ultimate load of the column, the ultimate load of NACFST column was 11.5% higher than that of RACFST column without steel fiber and silica fume. Simultaneously, for NACFST column, on the test day, the axial compressive strength of the ordinary concrete was 17.1% higher than that of the recycled aggregate concrete containing 100% RCA. The decrease in the axial load of RAC filled outer tube can be attributed to the lower strength of the recycled aggregate concrete as compared to the ordinary concrete.

The ultimate load of RACFST columns produced by additions of silica fume and 0.5%, 1.0% and 1.5% steel fiber were 17.6%, 16.4% and 18.9% higher respectively than that of RACFST column without additions. And the ultimate loads of RACFST columns were higher than that of NACFST column. The filling effect and pozzolanic action of silica fume and the confinement effect of steel fiber could be used to improve the ultimate load of RACFST columns.

3.3 Axial load-strain curves

To evaluate the effects of the tested parameters on the axial behavior of RACFST columns, the axial load-strain curves for specimens are shown in Fig. 3. The axial strain is the ratio of average value of the two LVDTs and the length of the column, and here axial strain is an absolute value. The hoop strain averaged from 4 horizontal strain gauges placed at specimen mid-height outside the steel tube. The axial strains corresponding to the ultimate load are shown in

Table 4. The results indicate that the additions have little effect on the axial strain corresponding to the ultimate load. The axial load-axial strain curves for all specimens experienced a softening stage after reaching the ultimate load.

The axial load-axial strain curves have in general almost a linear elastic region up to the ultimate load, after which the load dropped insignificantly. All RACFST columns maintained the load with an excellent ductility up to failure. The descending branch of RACFST columns with silica fume and steel fiber dropped not significantly compared to that of RACFST columns without additions. Compared with others, the curves of the RACFST columns with silica fume and 1.0% or 1.5% steel fiber began to ascend again after a descending branch, and the minimum load of the descending branch is higher than 85% of the ultimate load. It indicates that silica fume and steel fiber were used together in the columns will improve the ductility of the RACFST columns.

The hoop strain, measured by four horizontal strain gauges reflects the local deformation of steel tube in hoop direction under compressive load. The axial load-hoop strain curves show that the expansion of steel tube is very small until load is closed to the ultimate load, then the expansion of the steel tube rapidly develop.

The area between the axial load-axial strain curves till 85% of the ultimate load in the descending branch and the X axis is the energy dissipation capacity of the columns. For specimens C-100-1.0 and C-100-1.5, the minimum load of the descending branch was used to calculate the energy dissipation capacity, since the minimum load of the descending branch is higher than 85% of the ultimate load. The calculated energy dissipation capacity is shown in Fig. 4. Compare to the specimen C-100-0, the energy dissipation capacity of the RACFST specimens with silica fume and 0.5%, 1.0% and 1.5% steel fibers obtain enhancements of 43.2%, 85.7% and 188.9%, respectively. The energy dissipation capacity of RACFST specimens with 1.0% and 1.5% steel fibers and silica fume exceed that of NACFST specimen.

The concrete core without additions maintains the resistance to the applied axial load depends on the shear and friction on the cracked planes. Due to the bridging effect of the steel fibers crossing the concrete cracks, steel fibers

provides additional shear-frictional resistance to the sliding and allows the transfer of shear forces across the cracked planes. Silica fume enhances the strength of the transition zone in concrete while the steel fibers act as crack arrestors. So the addition of silica fume and steel fiber can improve the ductility and energy dissipation capacity of RACFST column.

3.4 The initial modulus

The initial modulus is defined as initial slope of the

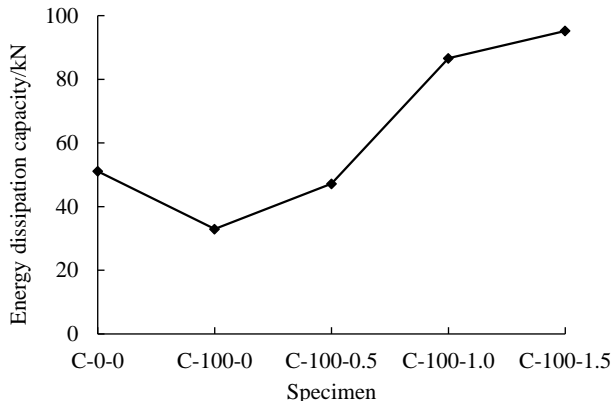


Fig. 4 Energy dissipation capacity of specimens

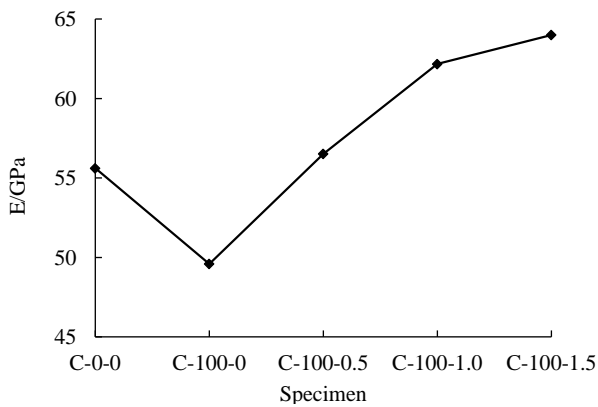


Fig. 5 Initial modulus of specimens

axial stress-axial strain curve. It is calculated as the ratio of 0.3 times ultimate stress to corresponding strain. The initial modulus of specimens (E) is shown in Fig. 5.

The results indicate that the NCA all replaced by recycled aggregate will decrease the initial modulus of column. An increase in the initial modulus of the RACFST columns was obtained by using silica fume and steel fibers together. The increases in the initial modulus of the columns with additions were 14%, 25.4% and 29% for the 0.5%, 1.0% and 1.5% steel fiber contents, respectively.

3.5 Axial strength of confined concrete

The silica fume plays its strengthening effect by increasing bond strength of cement paste–aggregate interface by means of filling effect and pozzolonic activity of silica fume. The main contribution of steel fibers to concrete can be seen after matrix cracking. Steel fibers randomly distributed in the matrix behave as crack arrestors by bridging mechanism. The strengthening effect of steel fiber will be decreased with the confining of steel tube. When the column is approaching the ultimate load, the lateral expansion of concrete becomes greater. The maximum radial pressure can be expressed by the semi-empirical relation (Tang *et al.* 1996)

$$p = (v_1 - v_2) \left(\frac{t}{R-t} \right) f_y \tag{1}$$

where t is the thickness of steel tube, R its outer radius and f_y its yield stress. Furthermore, v_1 and v_2 are the Poisson's ratios of the steel tube with and without filled-in concrete, respectively, at the ultimate stage. Ratio v_2 is taken as equal to 0.50 at the maximum strength point. Ratio v_1 is given by

$$v_1 = 0.2312 + 0.3582k - 0.1524 \left(\frac{f_c}{f_y} \right) + 4.843k \left(\frac{f_c}{f_y} \right) - 9.169 \left(\frac{f_c}{f_y} \right)^2 \tag{2}$$

where k is a factor of geometry of the form

Table 4 Test results of specimens

Specimens	E (GPa)		ϵ		N_u (KN)		f_c (MPa)	f'_c (MPa)	f'_c/f_c
	Calculated	Avg.	Experimental	Avg.	Experimental	Avg.			
C-0-0	60.52	55.62	0.0106	0.010	1486.4	1464.2	60.17	73.72	1.23
	50.72		0.01		1441.9				
C-100-0	46.65	49.6	0.01262	0.012	1338.8	1293.4	49.89	59.96	1.20
	53.87		0.0085		1248.0				
C-100-0.5	59.18	56.52	0.0104	0.011	1535.0	1521.0	55.36	78.53	1.42
	53.87		0.0121		1507.0				
C-100-1.0	70.36	62.18	0.0115	0.012	1448.3	1506.8	61.29	77.38	1.26
	54		1565.2						
C-100-1.5	67.5	64.0	0.0128	0.012	1559.1	1538.0	60.11	79.9	1.33

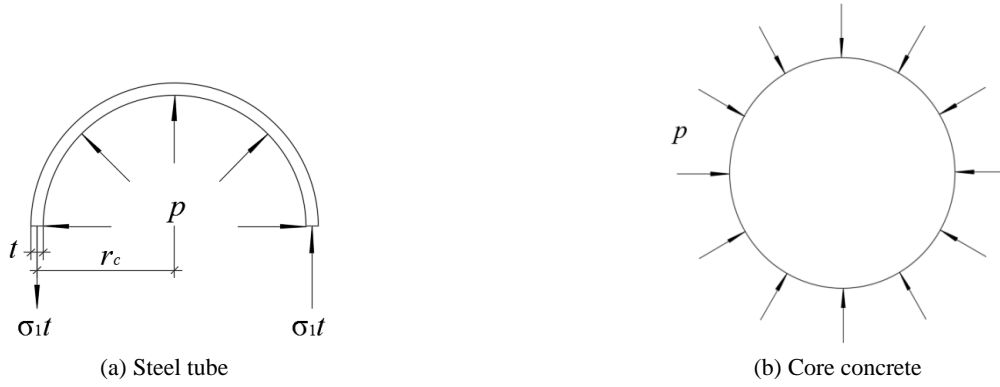


Fig. 6 Stress of steel tube and core concrete

$$k = 0.4011 + 3.9060 \times 10^{-2} \left(\frac{r}{t} \right) - 1.0320 \times 10^{-3} \left(\frac{r}{t} \right)^2 + 7.0480 \times 10^{-6} \left(\frac{r}{t} \right)^3 \quad (3)$$

The above equations are valid for (f_c/f_y) ranging from 0.04 to 0.20 for most of the practical applications.

The steel tube is stressed biaxially and the concrete core triaxially, the stress station of them showed in Fig. 6.

Where r_c is the distance from the center to the mid depth of the tube, σ_1 is the hoop tensile stress and given by

$$\sigma_1 = \frac{r_c}{t} p = \frac{r_c (v_1 - 0.5)}{R - t} f_y \quad (4)$$

the hoop tensile stress σ_1 and the longitudinal compressive stress σ_3 of the steel tube at the ultimate state satisfy the von Mises yield criterion given by

$$\sigma_1^2 - \sigma_1 \sigma_3 + \sigma_3^2 = f_y^2 \quad (5)$$

Substituting for σ_1 from Eq. (4) into Eq. (5), we have

$$\sigma_3 = \frac{\sigma_1 + \sqrt{4f_y^2 - 3\sigma_1^2}}{2} = \frac{(v_1 - 0.5)r_c + \sqrt{4(R-t)^2 - 3r_c^2(v_1 - 0.5)^2}}{2(R-t)} \quad (6)$$

based on the ultimate equilibrium theory, the ultimate load N_u can be described as the summation of the axial strength of the concrete core and the steel tube at the ultimate state, as shown in Eq. (7)

$$N_u = A_s \sigma_3 + A_c f'_c \quad (7)$$

substituting for σ_3 from Eq. (6) into Eq. (7), we have

$$f'_c = \frac{N_u - A_s \sigma_3}{A_c} \quad (8)$$

The values of f'_c are determined with N_u and shown in Table 4. The ratio of f'_c and f_c showed in Table 4 and Fig. 7

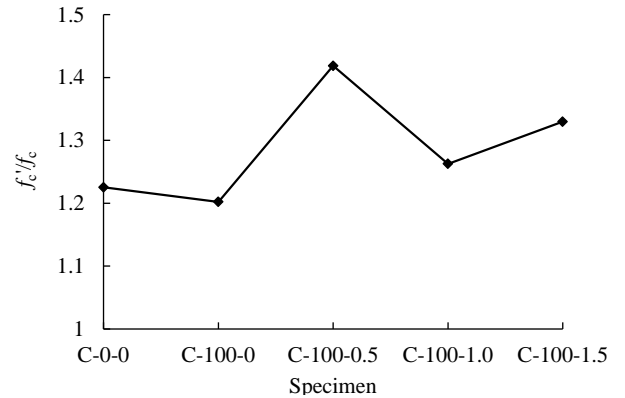
Fig. 7 Ratio of f'_c/f_c of specimens

Table 5 Comparison of ultimate strength between calculated results and test ones

Specimen	N_T	$N_{BS\ 5400}$	$N_{BS\ 5400}/N_T$	N_{AII}	N_{AII}/N_T	N_{EC4}	N_{EC4}/N_T	$N_{AISC-LRFD}$	$N_{AISC-LRFD}/N_T$
C-0-0	1464.2	1587.6	1.227	1171.5	0.906	1350.9	1.044	1030.9	0.797
C-100-0	1293.4	1699.2	1.161	1282.7	0.876	1473.3	1.006	1140.9	0.779
C-100-0.5	1521.0	1647.1	1.083	1230.7	0.809	1416.0	0.931	1089.5	0.716
C-100-1.0	1506.8	1711.4	1.136	1294.8	0.859	1486.7	0.987	1152.8	0.765
C-100-1.5	1538.0	1698.6	1.104	1282.1	0.834	1472.6	0.957	1140.2	0.741
Mean			1.14		0.86		0.94		0.83
COV			0.04		0.04		0.04		0.04

ranges from 1.20 to 1.42. The value of f_c'/f_c did not increase with the steel fiber volume percentages, it achieved the maximum value when the steel fiber volume percentage was 0.5%. The value of f_c'/f_c of the silica fume and steel fiber-reinforced columns increased compared with those without additions. The results showed that introducing silica fume and steel fiber at a 0.5%, 1.0% and 1.5% volume fraction increased the value of f_c'/f_c by 18.3%, 5% and 10.8% respectively for RACFST column C-100-0.

3.6 Predictions of the load capacity

In order to use the existing methods to predict the load capacity of RACFST column, the ultimate load of the specimens tested in this paper were firstly discussed in this section. The ultimate load for the RACFST specimens was compared to the design rules specified by BS5400 (2005), AIJ (Architectural Institute of Japan 1997), EC4 (Eurocode 2004) and AISC360 (ANSI/AISC 2005), as shown in Table 5. Among all the approaches recommended in current design codes, the method in EC4 gives the most satisfactory estimation. The mean value and COV of N_{EC4}/P_T are 0.94 and 0.04 respectively. Therefore EC4 can be adopted as the basic form to predict the column strength. The formula in EC4 can be used to calculate the load capacity of short RACFST columns. The cross-section capacity N_u of CFST column in EC4 is given in Eq. (9).

$$N_u = \eta_s f_y A_s + \left(1 + \eta_c \frac{f_y}{D f_c}\right) f_c A_c \quad (9)$$

in which η_s is the steel reduction factor and η_c is the concrete enhancement factor. Here the steel reduction and the concrete enhancement factors are evaluated as follows

$$\eta_s = 0.25(3 + 2\bar{\lambda}) \leq 1.0 \quad (10)$$

$$\eta_c = 4.9 - 18.5\bar{\lambda} + 17\bar{\lambda}^2 \geq 0 \quad (11)$$

the relative slenderness ratio $\bar{\lambda}$ is given by

$$\bar{\lambda} = \sqrt{\frac{f_y A_s + f_c A_c}{N_{cr}}} \quad (12)$$

here N_{cr} is Euler critical load, it is evaluated as follows

$$N_{cr} = \frac{\pi^2 (EI)_e}{L^2} \quad (13)$$

in which $(EI)_e$ is the effective stiffness of the member which is given by

$$(EI)_e = E_s I_s + K_e E_c I_c \quad (14)$$

where I_s is moment of inertia of steel tube and I_c is moment of inertia of concrete core. K_e is a correction factor equal to 0.6. E_s is the elastic modulus of steel and E_c is the elastic

modulus of concrete defined by

$$E_c = 22000 \left(\frac{f_c + 8MP_a}{10} \right)^{0.3} \quad (15)$$

4. Conclusions

This paper has presented the results of an experimental study on the behavior of the influence of silica fume and steel fibers on the axial compressive behavior of recycled concrete-filled steel tube columns. Based on the discussions and results presented in this study, the following conclusions can be drawn:

- Adding silica fume and steel fiber into core concrete has no effect on the failure mode of the recycled concrete-filled steel tube columns.
- Combined use of silica fume and steel fiber reinforcement can increase the ultimate load and initial modulus of the recycled concrete-filled steel tube columns. Modified by the silica fume and steel fiber, the ultimate load and initial modulus of recycled concrete-filled steel tube columns with 100% coarse aggregate are higher than that of normal concrete-filled steel tube column.
- The steel fiber play its effect after the cracks occur, so the addition of silica fume and steel fiber has little effect on the strain corresponding to ultimate load. The addition of silica fume and steel fiber can improve the ductility and energy absorption of recycled concrete-filled steel tube columns.
- Four design codes were used to predict the column strengths for recycled concrete-filled steel tube columns in this experiment. It was found that the column strengths by EC4 were closest to the test results. The calculated column strengths and test ones had a close agreement. The formula in EC4 can be used to calculate the load capacity of the short recycled concrete-filled steel tube columns.

Acknowledgments

The research described in this paper was financially supported by the youth fund of Yangtze University (2016cqn01). The authors greatly appreciate their financial support.

References

- Agrela, F., Barbudo, A., Ramírez, A., Ayuso, J., Carvajal, M.D. and Jiménez, J.R. (2012), "Construction of road sections using mixed recycled aggregates treated with cement in Malaga, Spain. Resources", *Conserv. Recycl.*, **58**, 98-106.
- ANSI/AISC 360-05 (2005), Specification for Structural Steel Buildings, American Institute of Steel Construction; Chicago, IL, USA.
- Architectural Institute of Japan (1997), Recommendations for Design and Construction of Concrete Filled Steel Tubular

- Structures, Architectural Institute of Japan; Tokyo, Japan.
- BS 5400 (2005), Steel concrete and composite bridges-Part5: Code of practice for design of composite bridges; London, UK.
- Chen, J. (2011), "Static behavior of recycled aggregate concrete filled steel tubular stub columns under axial compressive loading", Harbin Institute of Technology, Harbin, China. [In Chinese]
- Chen, Z.P., Chen, X.H., Ke, X.J. and Xue, J.Y. (2010a), "Experimental study on the mechanical behavior of recycled aggregate coarse concrete-filled square steel tube column", *Proceedings of 2010 International Conference on Mechanic Automation and Control Engineering*, pp. 1113-1116.
- Chen, Z.P., Liu, F., Zheng, H.H. and Xue, J.Y. (2010b), "Research on the bearing capacity of recycled aggregate concrete-filled circle steel tube column under axial compression loading", *Proceedings of 2010 International Conference on Mechanic Automation and Control Engineering*, **26**(Suppl 2), 1198-1201.
- Chen, Z.P., Zheng, S.F., Li, Q.L., Xue, J. and Chen, B. (2012), "Experimental study on behavior of recycled aggregate concrete filled square steel tubular long columns under eccentric compression loading", *J. Build. Struct.*, **33**(9), 21-29. [In Chinese]
- Chen, Z.P., Jing, C.G., Xu, J.J. and Zhang, X.G. (2017), "Seismic performance of recycled concrete-filled square steel tube columns", *Earthq. Eng. Eng. Vib.*, **16**(1), 119-130.
- Engelsen, C.J., Wibetoe, G., van der Sloot, H.A., Lund, W. and Petkovic, G. (2012), "Field site leaching from recycled concrete aggregates applied as sub-base material in road construction", *Sci. Total Environ.*, **427-428**, 86-97.
- Engelsen, C.J., van der Sloot, H.A. and Petkovic, G. (2017), "Long-term leaching from recycled concrete aggregates applied as sub-base material in road construction", *Sci. Total Environ.*, **587-588**, 94-101.
- Eurocode (2004), Design of steel and concrete structures. Part 1: General rules and rules for building, European Committee for Standardization; Brussels, Belgium.
- Konno, K., Sato, Y., Kakuta, Y. and Ohira, M. (1997), "The property of recycled concrete column encased by steel tube subjected to axial compression", *Transact. Japan Concrete Inst.*, **19**, 351-358.
- Konno, K., Sato, Y., Uedo, T. and Ohira, M. (1998), "Mechanical property of recycled concrete under lateral confinement", *Transact. Japan Concrete Inst.*, **20**, 287-292.
- Lotfy, A. and Al-Fayez, M. (2015), "Performance evaluation of structural concrete using controlled quality coarse and fine recycled concrete aggregate", *Cement Concrete Compos.*, **61**, 36-43.
- Ma, J. and Wang, Z.B. (2012), "Experimental Study on Bearing Capacity of Recycled Concrete-filled Circular Steel Tubular Columns under Axial Compression", *J. Guizhou Univ. (Natural Sciences)*, **29**(3), 104-107. [In Chinese]
- Manzi, S., Mazzotti, C. and Bignozzi, M.C. (2013), "Short and long-term behavior of structural concrete with recycled concrete aggregate", *Cement Concrete Compos.*, **37**, 312-318.
- Mas, B., Cladera, A., Del Olmo, T. and Pitarch, F. (2012), "Influence of the amount of mixed recycled aggregates on the properties of concrete for non-structural use", *Constr. Build. Mater.*, **27**(1), 612-622.
- Niu, H.C. and Cao, W.L. (2015), "Full-scale testing of high-strength RACFST columns subjected to axial compression", *Magaz. Concrete Res.*, **67**(5), 257-270.
- Rodríguez, C., Parra, C., Casado, G., Miñano, I., Albaladejo, F., Benito, F. and Sánchez, I. (2016), "The incorporation of construction and demolition wastes as recycled mixed aggregates in non-structural concrete precast pieces", *J. Cleaner Prod.*, **127**, 152-161.
- Seara-Paz, S., González-Fontboa, B., Martínez-Abella, F. and González-Taboada, I. (2016), "Time-dependent behaviour of structural concrete made with recycled coarse aggregates. Creep and shrinkage", *Constr. Build. Mater.*, **122**, 95-109.
- Tang, J., Hino, S., Kuroda, I. and Ohta, T. (1996), "Modelling of stress-strain relationships for steel and concrete in concrete filled circular steel tubular columns", *Steel Constr. Eng.: JSSC*, **3**(11), 35-46.
- Thomas, C., Setián, J. and Polanco, J.A. (2016), "Structural recycled aggregate concrete made with precast wastes", *Constr. Build. Mater.*, **114**, 536-546.
- Qiu, C.C., Wang, Q.Y., Shi, X.S. and Yang, W.X. (2011), "Experimental investigation on the behavior of recycled concrete-filled thin-walled steel tube under axial compression", *J. Experim. Mech.*, **26**(1), 8-15. [In Chinese]
- Wang, Y.Y., Chen, J. and Geng, Y. (2015), "Testing and analysis of axially loaded normal strength recycled aggregate concrete filled steel tubular stub columns", *Eng. Struct.*, **86**, 192-212.
- Wu, B., Zhao, X.Y. and Zhang, J.S. (2012), "Cyclic behavior of thin-walled square steel tubular columns filled with demolished concrete lumps and fresh concrete", *J. Constr. Steel Res.*, **77**, 69-81.
- Wu, B., Zhao, X.Y., Zhang, J.S. and Yang, Y. (2013), "Cyclic testing of thin-walled circular steel tubular columns filled with demolished concrete blocks and fresh concrete", *Thin-Wall. Struct.*, **66**, 50-61.
- Xu, J.J., Chen, Z.P., Xue, J.Y., Chen, Y.L. and Zhang, J.T. (2017), "Simulation of seismic behavior of square recycled aggregate concrete - filled steel tubular columns", *Constr. Build. Mater.*, **149**, 553-566.
- Yang, Y.F. and Han, L.H. (2006a), "Compressive and flexural behavior of recycled aggregate concrete filled steel tubes (RACFST) under short-term loadings", *Steel Compos. Struct., Int. J.*, **6**, 257-284.
- Yang, Y.F. and Han, L.H. (2006b), "Experimental behavior of recycled aggregate concrete filled steel tubular columns", *J. Constr. Steel Res.*, **62**, 1310-1324.
- Yang, Y.F., Han, L.H. and Zhu, L.T. (2009), "Experimental performance of recycled aggregate concrete-filled circular steel tubular columns subjected to cyclic flexural loadings", *Adv. Struct. Eng.*, **12**(2), 183-194.
- Zhang, J.S. (2011), "Experimental study on axial and seismic behaviors of square thin-walled steel tubular columns filled with demolished concrete lumps", Master Dissertation; South China University of Technology, Guangzhou, China.
- Zhang, X.G., Chen, Z.P., Xue, J.Y., Su, Y.S. and Fan, J. (2012), "Experimental study and mechanical behavior analysis of recycled aggregate concrete filled steel tubular long columns under axial compression", *J. Build. Struct.*, **33**, 12-20. [In Chinese]
- Zhang, X.G., Chen, Z.P., Xue, J.Y. and Su, Y.S. (2014), "Experimental study on seismic behavior of recycled aggregate concrete filled steel tube columns", *China Civil Eng. J.*, **47**(9), 45-56. [In Chinese]